Mesoporous Materials

Cubic Mesoporous Frameworks with a Mixed Semiconductor Nanocrystalline Wall Structure and Enhanced Sensitivity to Visible Light**

Michael H. Bartl, Stefan P. Puls, Jing Tang,
Helga C. Lichtenegger, and Galen D. Stucky*

Since the discovery of mesostructured materials in the early 1990s[1] a great deal of effort has been devoted to developing new structures, compositions, and functionalities.[2] The ability to synthesize semiconducting single- or multicomponent metal-oxide mesostructured materials with controlled morphologies[3] has been a major step towards functional materials with potential applications in sensing, catalysis, and optoelectronics.[4] We describe herein the synthesis and properties of a new generation of ordered mesostructured composites with mesopore walls composed of integrated 3D arrays of different types of wide and narrow band-gap semiconductor nanocrystals including oxides, sulfides, and selenides. Such an integrated 3D coassembly of different functional units is of great importance for optoelectronic applications that rely on the transfer of electrons or holes between two or more active components. Examples of such systems are sensitized titania solar cells and photocatalysts, for which it has been shown that solar conversion efficiency can be strongly increased in the presence of sensitizing dye molecules or narrow band-gap semiconductor nanocrystals.[5] Fabrication techniques previously developed for such functionalized composite titania materials are based on step-by-step methods in which organic molecules or premade semi-

[*] Dr. M. H. Bartl, S. P. Puls, Dr. H. C. Lichtenegger,
Prof. Dr. G. D. Stucky
Department of Chemistry and Biochemistry
University of California, Santa Barbara
Santa Barbara, CA 93106 (USA)
Fax: (+1) 805-893-4120
E-mail: stucky@chem.ucsb.edu

J. Tang, Prof. Dr. G. D. Stucky
Materials Department
University of California, Santa Barbara
Santa Barbara, CA 93106 (USA)

Dr. H. C. Lichtenegger
Institut für Werkstoffkunde und Materialprüfung
Technische Universität Wien
1140 Wien (Austria)

conductor nanocrystals are grafted or deposited onto the surface of beforehand patterned titania film matrices.[6] In contrast, the mixed nanocrystalline anatase titania/cadmium chalcogenide mesoporous films presented here are prepared by a fast and inexpensive single-run supramolecular templating route based on acidic sol–gel chemistry. By selectively using competing molecular self-assembly, phase transitions and stabilities as well as crystallization kinetics, we are able to combine synthesis, assembly, and patterning into a one-pot single-precursor dip-coating process followed by heat treatment of the samples with varying gas/vapor atmospheres.

The mesoporous composite films were prepared by dip-coating from a highly acidic solution containing titanium(IV)-ethoxide and cadmium chloride as precursors for the wide or narrow band-gap nanocrystalline semiconductors, respectively, and a non-ionic triblock copolymer as the mesostructure-directing species. It has been shown that under highly acidic conditions, the hydrolyzed titania nanoentities are not prone to cross-link and can be stabilized over an extended period of time. This gives the structure-directing surfactant enough time to assemble into its most stable thermodynamic phase, which is determined primarily by the temperature and the volume ratio of inorganic species to surfactant.[3d,e] For the volume ratio of Cd/Ti to surfactant used here, a stable cubic mesostructural order was obtained by storing the dip-coated films at 10°C. The films were then subjected to an extended heat–gas/vapor treatment during which they changed from a liquid-crystalline hybrid organic–inorganic mesostructured composite to a mesoporous framework built up of integrated arrays of different semiconductor nanocrystals. The films were first kept in an oxidative high-temperature environment to remove the surfactant and promote condensation of the solubilized titania nanoentities, followed by nucleation and growth of semiconducting anatase nanocrystals out of the amorphous titania matrix. Simultaneously, the coassembled molecular cadmium species separates into cadmium oxide nanoclusters, which are evenly distributed in the titania framework in accordance with previous studies of sol–gel matrices doped with transition-metal ions.[7] By changing the processing conditions to an S- or Se-vapor atmosphere diluted with an inert gas, these cadmium oxide nanoclusters are then selectively converted into crystalline semiconducting CdS or CdSe nanoparticles through a redox-coupled ion-exchange reaction mechanism.[8] After only a few minutes of exposure to S or Se vapor, the films became yellow or orange (Figure 1 f), indicating the successful transformation of cadmium oxide into its nanocrystalline sulfide or selenide analogues.

The mesostructural order and wall composition of the final films were determined by high-resolution scanning electron microscopy (HRSEM) and transmission electron microscopy (TEM) in combination with energy dispersive X-ray spectroscopy (EDX). The body-centered-cubic (bcc) mesopore arrangement was confirmed by TEM imaging along the [100] and [111] crystallographic axes. Representative TEM micrographs demonstrate the high mesostructural order of both the titania–CdSe (Figure 1 a and b) and titania–CdS (Figure 1 c) composite films. Additionally, HRSEM imaging reveals a completely open-pore surface of the film
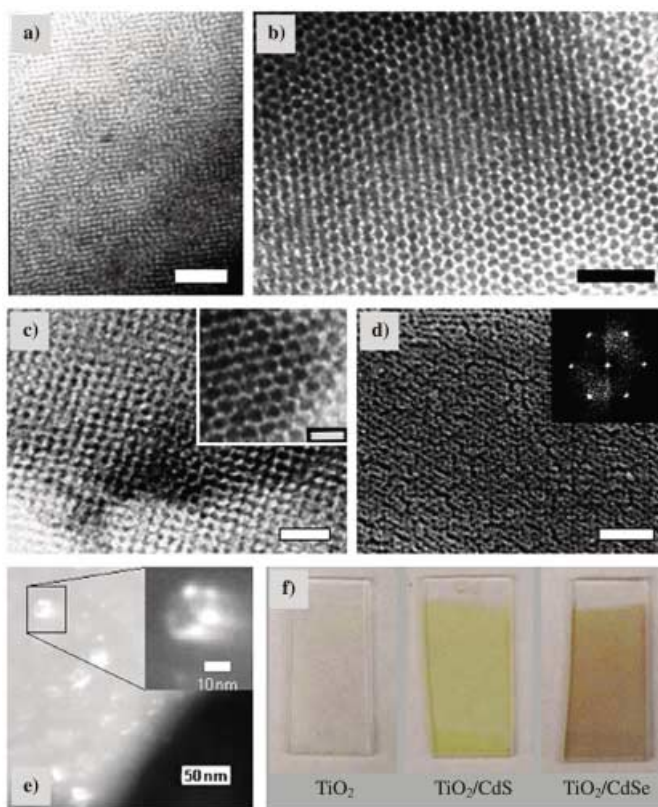
Figure 1. Electron micrographs and optical photographs of cubic mesoporous nanocrystalline anatase titania/cadmium chalcogenide composite films. a–c) TEM images of titania/CdSe, (a and b), and titania/CdS (c) thin films. Images shown in a) and c) were recorded along the [100] zone axis, whereas image b) and the inset of c) give a view along the [111] zone axis of the bcc symmetry. d) SEM image of the open-pore surface of a titania/CdS film (inset shows the Fourier transform of the open-pore symmetry). e) Bragg-contrast image in dark field TEM of a titania/CdS sample showing individual nanocrystals scattering in the off-centered objective aperture. f) Photographs of mesoporous pure titania and composite titania/cadmium chalcogenide films. The scale bars are 100 nm in Figure a) and d), 50 nm in Figure b) and c), and 20 nm in the inset of Figure c).

(Figure 1 d) with the [111] direction of the bcc mesopore symmetry running perpendicular to the film surface, as indicated by the hexagonal Fourier pattern (Figure 1 d inset). This image confirms that the continuously cubic ordered and interconnected mesoporous framework is extended throughout the film and thus fully accessible from the surface, which is a particular important property with respect to infiltration of the mesoporous framework with, for example, hole-conducting conjugated polymers.[9] Furthermore, from quantitative EDX analysis we found a homogeneous cadmium distribution within the mesopore walls (Cd:Ti molar ratios are the same as in the respective precursor solutions) and a constant Cd:S or Cd:Se ratio of unity, thus indicating a quantitative oxygen–chalcogenide exchange during the S or Se vapor treatment.

We studied the crystallinity of the composite mesoporous framework by Bragg-contrast imaging in dark-field TEM and XRD analysis. Individual nanocrystals (3–6 nm in size) can be

imaged in Bragg contrast in the form of bright spots at various places within the mesoporous framework walls (Figure 1e). The position of illuminated spots changes quickly upon tilting as different lattice planes of the various crystallites fulfill the diffraction condition and therefore diffract into the off-centered objective aperture. Both the type and structure of these nanocrystals were investigated by means of XRD. Figure 2 shows a comparison of the diffraction patterns of a nondoped titania mesoporous film (pattern A) and those doped with Cd and treated with either S or Se vapor (patterns B and C, respectively). While the diffraction peaks obtained from the nondoped films can be indexed according to an anatase phase, the patterns of the two composite films exhibit a number of additional diffraction peaks (Figure 2a), which can all be assigned to reflections that are typical for a CdS and CdSe wurtzite structure (Figure 2b). Due to the small size of the anatase, CdS, and CdSe crystallites, all of the diffraction peaks are strongly broadened. By applying the Scherrer formula to the peak widths of selected reflections (deconvoluted with standard peak fitting routines), we estimated the size of the crystallites to be between 4 and 7 nm.

To test for cooperative functionality of our nanocrystalline composite mesoporous films we measured their visible-light photocatalytic activity. CdS nanocrystals are known to have a sensitizing effect on titania, since they combine a high absorption cross section for visible light with an energy-band structure that allows injection of the photoexcited electrons into the titania conduction band,[6b,d,10] from where they are transferred along the mesoporous framework by a hopping mechanism, which is typical for nanocrystalline anatase titania composites.[5a] We analyzed the solar sensitization efficiency of our nanocrystalline mixed anatase titania–CdS mesoporous composite films of 200 to 300 nm thickness by comparing their ability to generate a visible-light photocurrent (I_{ph}) with that of pure anatase titania mesoporous films. The setup for these measurements was a standard two-electrode photoelectrochemical cell working in non-regenerative mode as described elsewhere.[5a] To compensate for small deviations from the sample and setup, such as film thickness and roughness or angle of incident light, all measurements were done in two steps. First we determined the I_{ph} response to UV and visible photons simultaneously (UV + vis) and used this value as maximum photoinducible I_{ph} under the given illumination, since in this case the whole film (anatase and CdS) is able to absorb light. The effect of visible-light sensitization expressed as the I_{ph} response to visible photons only (vis-only) was then determined with the same setup by blocking the UV photons with a 400 nm longpass filter. Typical experimental results for pure anatase titania and composite anatase titania/CdS (5 mol% CdS) mesoporous films are given in Figures 3a and b, respectively. As expected, both samples exhibit a well-defined periodic on/off I_{ph} response to the light/dark modulated UV + vis illumination (left part of response curves). However, by switching from UV + vis to vis-only illumination (right part of
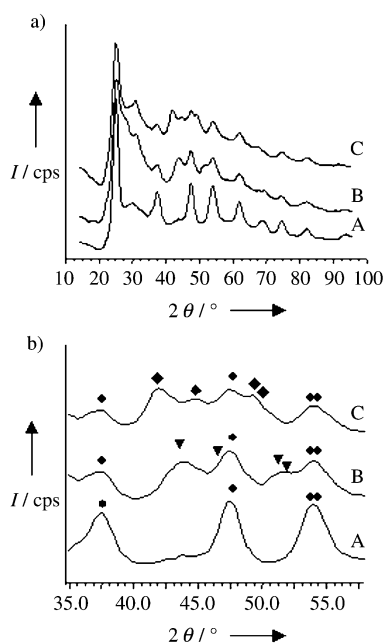
Figure 2. a) X-ray diffraction patterns of cubic mesoporous nanocrystalline pure anatase titania (pattern A) and composite nanocrystalline anatase titania/CdS (pattern B) and anatase titania/CdSe (pattern C) film samples. The diffracted intensities were plotted versus scattering angles $2\theta_{Cu}$ as would be observed with Cu$_{K\alpha}$ radiation, for better comparison with the literature. The initially obtained scattering angles $2\theta_{Mo}$ from the measurement with Mo$_{K\alpha}$ radiation were converted to $2\theta_{Cu}$ according to $\theta_{Cu} = \arcsin(\lambda_{Cu}/\lambda_{Mo} \sin\theta_{Mo})$, where λ_{Cu} and λ_{Mo} are the wavelengths of Cu$_{K\alpha}$ and Mo$_{K\alpha}$ radiation, respectively. b) Detailed comparison in the range 35 to 58° of $2\theta_{Cu}$ of the three diffraction patterns; dots indicate the (004), (200), and (105/211) reflections of the anatase nanocrystals; triangles and diamonds mark the (110), (103), (112), and (201) wurtzite reflections of the CdS and CdSe nanocrystals, respectively. Patterns are offset in X-ray intensity I.
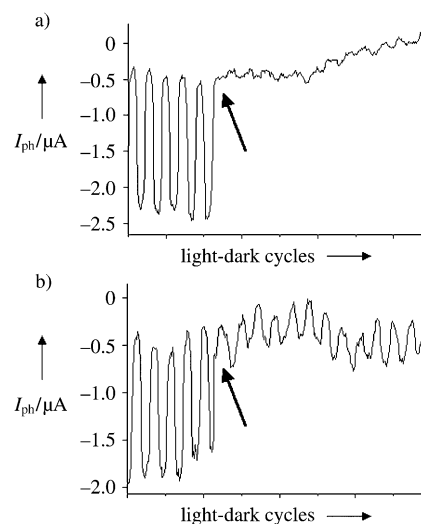
Figure 3. Periodic on/off photocurrent I_{ph} response curves of a) nanocrystalline pure anatase titania and b) nanocrystalline composite anatase titania/CdS cubic mesoporous films deposited on fluorinated tin oxide conducting glass electrodes and illuminated with a periodically light/dark modulated xenon lamp; arrows indicate the switching from illumination with UV and visible photons simultaneously (left side of the arrow) to illumination with visible photons only (right side of the arrow).

response curves), the pure anatase titania mesoporous films failed to produce a measurable I_{ph}, whereas the composite anatase titania–CdS mesoporous film was still able to generate a clear on/off I_{ph} response, which is around 25% of the total UV+vis I_{ph}. It should be emphasized that the conservation of 25% of the maximum photoinducible current under vis-only illumination is exceptionally high and points to an efficient intrinsic visible-light-sensitization effect, considering that under vis-only excitation only the 5% CdS portion of the film contributes to the absorption process. These first results are very promising and we are currently exploring sensitization effects in a number of new mesoporous titania composites with integrated zinc-, lead-, and silver chalcogenide nanocrystals.

In this work we have presented a novel approach for the simultaneous synthesis and 3D organization of different optoelectronically active species. The procedure is fast, inexpensive, and suitable to be integrated into large area device fabrication techniques. Our cubic mesoporous films have a highly crystalline wall structure composed of integrated arrays of wide and narrow band-gap semiconductor nanocrystals, as determined by a combination of several analytical methods. Furthermore, we demonstrated the cooperative functionality of these composite nanocrystalline materials by successful proof-of-principle visible-light sensitization of a cubic mesoporous anatase titania film with cadmium sulfide nanocrystals acting as sensitizing integral part of the mesopore wall structure. Given the generality and flexibility of sol–gel self-assembly chemistry the fabrication approach presented here opens the field to a multitude of new cooperatively functional materials with custom-made nanostructures and compositions.

Experimental Section

Appropriate amounts of anhydrous $CdCl_2$ were dissolved in HCl (2.7 mL, 12.1 M) before titanium(IV)ethoxide (3.9 mL) was added and hydrolyzed while the mixture was cooled with ice/water and vigorously stirred for 5 minutes (ratio of Cd to Ti was varied between 1 and 10 mol%). This mixture was combined with a solution of poly(ethylene oxide)$_{20}$-poly(propylene oxide)$_{70}$-poly(ethylene oxide)$_{20}$ surfactant (1 g; Pluronic P123, BASF) dissolved in ethanol (12 g) and stirred for another 10 minutes before thin films were prepared by dip-coating onto cleaned glass slides at a speed of 1 mm s^{-1}. The films were dried at room temperature and then stored for at least 6 h at 10°C. Calcination and sulfur or selenium vapor treatment were performed in a tube furnace. First the samples were heated in air to 400°C at 1°C min^{-1} and kept there for 5 h. Then the temperature was reduced to 250°C or 300°C at 5°C min^{-1} and around 3 g of elemental sulfur or selenium were placed in the tube in front of the samples under a slow argon gas stream. After 10 to 30 minutes of vapor treatment the remaining sulfur or selenium was removed from the tube and the films were heated under argon at 5°C min^{-1} to 350°C and held there for 15 minutes before they were allowed to cool down to room temperature at a rate of 10°C min^{-1}.

A JEOL 2000FX electron microscope operating at 200 kV was used for TEM imaging and EDX spectroscopy. HRSEM images were taken on a JEOL 6340F electron microscope. XRD measurements were done on a SMART diffractometer (Mo$_{K\alpha}$ radiation) equipped with a charge coupled device (CCD) detector. For the photocurrent I_{ph} measurements the mesoporous films with a thickness of 200 to 300 nm (as determined by cross-sectional SEM investigation) were deposited on fluorinated tin oxide conducting glass electrodes and immersed in a sodium acetate electrolyte solution (0.1 M) with a platinum counter electrode. The films were excited on an area of 0.25 cm^2 by the chopped (≈ 0.25 Hz) emission of a broadband xenon lamp (150 W). The light/dark short circuit I_{ph} response under zero bias was recorded with a Philips amperemeter.

[1] a) T. Yanagisawa, T. Shimizu, K. Kuroda, C. Kato, *Bull. Chem. Soc. Jpn.* **1990**, *63*, 988; b) C. T. Kresge, M. E. Leonowicz, W. J. Roth, J. C. Vartuli, J. S. Beck, *Nature* **1992**, *359*, 710.

[2] See for example: a) F. Schüth, W. Schmidt, *Adv. Mater.* **2002**, *14*, 629; b) J. Y. Ying, C. P. Mehnert, M. S. Wong, *Angew. Chem.* **1999**, *111*, 58; *Angew. Chem. Int. Ed.* **1999**, *38*, 56; c) C. J. Brinker, *Curr. Opin. Solid State Mater. Sci.* **1996**, *1*, 798; d) G. D. Stucky, Q. Huo, A. Firouzi, B. F. Chmelka, S. Schacht, I. G. Voigt-Martin, F. Schüth in *Progress in Zeolite and Microporous Materials, Studies in Surface Science and Catalysis, Vol. 105* (Eds.: H. Chon, S.-K. Ihm, Y. S. Uh), Elsevier, Amsterdam, **1997**, pp. 3–28; e) P. Behrens, *Angew. Chem.* **1996**, *108*, 561; *Angew. Chem. Int. Ed. Engl.* **1996**, *35*, 515.

[3] a) P. D. Yang, D. Y. Zhao, D. I. Margolese, B. F. Chmelka, G. D. Stucky, *Nature* **1998**, *396*, 152; b) D. Grosso, G. Soler-Illia, F. Babonneau, C. Sanchez, P. A. Albouy, A. Brunet-Bruneau, A. R. Balkenende, *Adv. Mater.* **2001**, *13*, 1085; c) Y. K. Hwang, K. C. Lee, Y. U. Kwon, *Chem. Commun.* **2001**, 1738; d) P. C. A. Alberius, K. L. Frindell, R. C. Hayward, E. J. Kramer, G. D. Stucky, B. F. Chmelka, *Chem. Mater.* **2002**, *14*, 3284; e) K. L. Frindell, M. H. Bartl, A. Popitsch, G. D. Stucky, *Angew. Chem.* **2002**, *114*, 1001; *Angew. Chem. Int. Ed.* **2002**, *41*, 959; f) F. Bosc, A. Ayral, P. A. Albouy, C. Guizard, *Chem. Mater.* **2003**, *15*, 2463.

[4] a) M. E. Davis, *Nature* **2002**, *417*, 813; b) B. J. Scott, G. Wirnsberger, G. D. Stucky, *Chem. Mater.* **2001**, *13*, 3140.

[5] a) M. Grätzel, *Nature* **2001**, *414*, 338; b) A. J. Nozik, *Phys. E* **2002**, *14*, 115.

[6] a) A. Hagfeldt, M. Grätzel, *Acc. Chem. Res.* **2000**, *33*, 269; b) R. Vogel, P. Hoyer, H. Weller, *J. Phys. Chem.* **1994**, *98*, 3183; c) A. Zaban, O. I. Micic, B. A. Gregg, A. J. Nozik, *Langmuir* **1998**, *14*, 3153; d) X. M. Qian, D. Q. Qin, Y. B. Bai, T. J. Li, X. Y. Tang, E. K. Wang, S. J. Dong, *J. Solid State Electrochem.* **2001**, *5*, 562; e) R. Plass, S. Pelet, J. Krueger, M. Grätzel, U. Bach, *J. Phys. Chem. B* **2002**, *106*, 7578; f) J. Tang, H. Birkedal, E. W. McFarland, G. D. Stucky, *Chem. Commun.* **2003**, 2278.

[7] M. Nogami, K. Nagaska, E. Kato, *J. Am. Ceram. Soc.* **1990**, *73*, 2097.

[8] L. Dloczik, R. Engelhardt, K. Ernst, S. Fiechter, I. Sieber, R. Könenkamp, *Appl. Phys. Lett.* **2001**, *78*, 3687.

[9] a) K. M. Coakley, Y. Liu, M. D. McGehee, K. L. Frindell, G. D. Stucky, *Adv. Funct. Mater.* **2003**, *13*, 301; b) K. M. Coakley, M. D. McGehee, *Appl. Phys. Lett.* **2003**, *83*, 3380.

[10] a) J. C. Yu, L. Wu, J. Lin, P. Li, Q. Li, *Chem. Commun.* **2003**, 1552; b) L. M. Peter, D. J. Riley, E. T. Tull, K. G. U. Wijayantha, *Chem. Commun.* **2002**, 1030; c) H. Fujii, M. Ohtaki, K. Eguchi, H. Arai, *J. Mol. Catal. A* **1998**, *129*, 61.